

Review

# Recent Progresses in Plasmonic Biosensors for Point-of-Care (POC) Devices: A Critical Review

Caterina Serafinelli <sup>1,2,3,4</sup> , Alessandro Fantoni <sup>1,3,\*</sup> , Elisabete C. B. A. Alegria <sup>1,2</sup>  and Manuela Vieira <sup>1,3,4</sup> 

<sup>1</sup> ISEL—Instituto Superior de Engenharia de Lisboa, 1949-014 Lisboa, Portugal; c.serafinelli@campus.fct.unl.pt (C.S.)

<sup>2</sup> Centro de Química Estrutural, Institute of Molecular Sciences, Instituto Superior Tecnico IST, Universidade de Lisboa, 1049-001 Lisboa, Portugal

<sup>3</sup> CTS—Centre of Technology and Systems, 2829-516 Caparica, Portugal

<sup>4</sup> DEE-FCT-UNL, Department of Electrotechnical and Computer Engineering of the Faculty of Science and Technology of the Universidade NOVA de Lisboa, 2829-516 Caparica, Portugal

\* Correspondence: afantoni@deetc.isel.ipl.pt

**Abstract:** The recent progresses in the research of plasmonic phenomena and materials paved the route toward the development of optical sensing platforms based on metal nanostructures with a great potential to be integrated into point-of-care (POC) devices for the next generation of sensing platforms, thus enabling real-time, highly sensitive and accurate diagnostics. In this review, firstly, the optical properties of plasmonic metal nanoparticles will be illustrated, whereafter the engineering of POC platforms, such as microfluidics and readout systems, will be considered with another critical point which is surface functionalization. Attention will also be given to their potential in multiplexed analysis. Finally, the limitations for effective implementation in real diagnostics will be illustrated with a special emphasis on the latest trend in developing cutting-edge sensing systems.

**Keywords:** POC devices; plasmonic biosensors; readout systems; multiplexed detection



**Citation:** Serafinelli, C.; Fantoni, A.; Alegria, E.C.B.A.; Vieira, M. Recent Progresses in Plasmonic Biosensors for Point-of-Care (POC) Devices: A Critical Review. *Chemosensors* **2023**, *11*, 303. <https://doi.org/10.3390/chemosensors11050303>

Academic Editors: Jingsong Li, Hao Deng and Maria Grazia Manera

Received: 17 March 2023

Revised: 5 May 2023

Accepted: 15 May 2023

Published: 19 May 2023



**Copyright:** © 2023 by the authors. Licensee MDPI, Basel, Switzerland. This article is an open access article distributed under the terms and conditions of the Creative Commons Attribution (CC BY) license (<https://creativecommons.org/licenses/by/4.0/>).

## 1. Introduction

The efforts made to design real-time assays reflect the exponentially growing interest in the fast and easy identification of many biomarkers for several diseases so that many lives can be saved thanks to the detection of a disease at an early stage as well as facilitating the management of more personalized and efficient therapies, aiming to develop and improve personalized medicine. With this in mind, fervent activity is directed towards the advancement of point-of-care (POC) devices [1]: these tests enable analysis using very small sample volumes with no or little preparation, providing results in shorter times compared to routine lab tests. They offer the additional advantage of being interpreted and implemented without any special equipment or training, while they are administered externally to hospitals and clinics practice, in a home environment. Furthermore, they are cost-effective and can be easily transported. The World Health Organization (WHO) defined the criteria that must be satisfied for an ideal diagnostic system that can be summarized by the ASSURED acronym: affordable, sensitive, specific, user-friendly, rapid, equipment-free and delivered to the end users [2]. To better understand the relevance of these characteristics, it is necessary to discuss the asymmetries of needs between developed and third-world countries. In developed countries, there is a need for decentralization in order to reduce the volume of present access to hospitals, freeing resources for properly determined cases. To make it possible, the essential activities of disease screening and monitoring for prevention purposes should be performed at home by the patient themselves or by untrained personnel. Access to these data could be provided to medical doctors through remote access, and the interpretation of such a large amount of data could be supported by an existing analytical approach. Proper detection of disease when still in an early stage and risk stratification

would be of great help in disease prevention and treatment, improving healthy-aging expectations. Differently, in remote regions, the needs are quite different. Hospitals are insufficient, in numbers and dimensions, and a great number of people have almost no access to any kind of healthcare, even when in great need and in situations of serious illness. Among the many problems that can be claimed as a cause for such a situation, we recall here one of them, which is common to most countries and not depending on the specific government model: the remote geographical location of patients, at large distances from the hospitals, in a rural environment [3]. Despite having very different natures, these two situations can be both addressed by the employment of new technologies for developing Point-of-Care (POC) systems. New technologies are employed to develop POC devices relying on lab-on-chip (LOC) hardware and remote connections based on Internet-of-Things (IoT) infrastructure. Lab-on-chip devices are detection systems based on microfluidics which integrate multiple procedures of a laboratory on a single chip of only a few square millimeters to a few square centimeters in size, in order to develop ‘from-sample-to-answer’ analytical systems where the input is a rough or low processed sample, and the output is a qualitative or quantitative evaluation of one or more required analytes. The design of an LOC device, thus, will take into account the various steps needed to perform the analysis: fluidic handling, molecular recognition, transduction, sample preparation, and signal amplification [4]. In addition, LOC devices, including their design and development, have been one of the most important tools in cancer research since their early existence due to the critical importance of clarifying the processes related to cancer, thus improving the speed, accuracy, and accessibility of diagnosis, resulting in earlier detection and better outcomes for patients [5]. With advancements in sensor technology, the Internet of Medical Things (IoMT) (also referred to as healthcare IoT) is emerging as a next-generation analytical tool, enabling the transition of health systems from a model based on hospitals to caring centred on the patient, by means of its ability to provide access anywhere during the progression of care. The objective of IoT technologies is to create a connection between smart devices incorporating systems, such as processors, sensors, and communication hardware, with each of them providing information and data in a single communication architecture [6]. Healthcare can be recognized among the main domains of application for IoT, making patients and clinicians closer through medical devices enabling remote access to cumulate, process and transmit medical data over a secure network, thus enhancing the involvement and satisfaction of the patient. In a standard clinical setting, healthcare solutions are provided by an IoT network made up of interconnected devices and dedicated to healthcare analysis, such as patient monitoring and automatic recognition of situations requiring medical assistance [7]. In addition, HIoT technologies create opportunities to increase the conventional approaches of diagnosis utilized by physicians [8]. Nowadays, in a further step towards the development of a novel biosensor, the research is focused on combining the innovative properties of plasmonic transducers with advanced microfluidic systems to improve upon the customary techniques and to produce miniaturized, user-friendly, automated, and portable instruments for POC applications, with the capability to perform a label-free and multiplexed (i.e., quantifying several analytes at the same time) analysis. During the last decades, metal nanoparticles have emerged as effective tools to detect different biomolecules with high precision and sensitivity. At the basis of the metal nanoparticles’ properties there are the collective oscillations of the free electrons and the extensive electric-field enhancement when exposed to light, which lead to different light-matter interactions such as localized surface plasmon resonance (LSPR) and surface-enhanced Raman scattering. Significantly, these nanoparticles display clear changes in the optical properties when they change shape as results of growth or etching, or when they aggregate or disaggregate or as results of variations in the dielectric environment around the particle surface. Further, some metal nanoparticles demonstrate enzyme-like activity, producing coloured products from colourless precursor, so that the colour changes generated from their properties represent an outstanding opportunity for colorimetric detection in user-friendly test and devices. In addition, taking advantage of the large

electromagnetic field confined around the surface enhancing the light scattering, metal nanoparticles opened the way to surface-enhanced Raman spectroscopy (SERS), a powerful technology to detect molecules with high sensitivity and accuracy down to the molecular level. According to its benefits, a straightforward idea is to integrate SERS analysis based on metal nanoparticles in POC devices able to obtain, in real-time, molecular information for sensing in a low-cost manner. In this scenario, according to real-time sensing arising from their optical properties (colour changes) and their use in SERS spectroscopy enabling powerful readout systems, plasmonic metal nanoparticles have attracted great interest in the design and development of POC devices during recent years. In this work, a critical discussion on the engineering along with the future scenario of POC platforms will be provided: Firstly, the optical properties of plasmonic nanoparticles, the basis of sensing, will be reviewed in Section 2. The engineering of POC devices will be reviewed starting from Section 3, where microfluidics will be discussed with a special emphasis on the traditional and most widespread technologies used in commercial POC devices, the lateral flow assay (LFA) and paper-based analytical devices ( $\mu$ PADs). The readout systems will be illustrated in Section 4, focusing on SERS analysis and smartphone-assisted devices, since they are the most promising technologies for implementation in real analysis. Furthermore, another critical point in the development of POC devices, metal surface functionalization, is reviewed in Section 5, along with its great potential in multiplexed analysis (Section 6). In Section 7, the applications deriving from the combination of various types of engineering such as, for example, LFA with different readout systems will be presented and classified into three categories: smartphone-assisted devices, liquid biopsy, and wearable plasmonic biosensing, according to their practical use. Finally, in Section 8, the summary of the work along with a critical discussion of the limiting factors of POC technology will be considered along with the future trends in the development of next-generation sensors.

## 2. Optical Properties of Plasmonic Metal Nanoparticles

When electromagnetic radiation, such as light, interacts with a metal surface, attractive surface excitations are generated. If the free electrons of a metal are coupled with the electromagnetic field of the radiation, thus oscillating in resonance, surface-bound modes, called surface plasmon resonances (SPRs) are originated. Frequently, the SPRs are classified into two categories: propagating surface plasmons (PSPs) and localized surface plasmons (LSPs) [9]. The first type consists of running surface waves called propagating surface plasmon resonances (PSPRs). Electromagnetic fields are associated with PSPRs: they penetrate the surrounding dielectric environment, thus providing a sensing probe resulting from its sensitivity to changes in a refractive index such as those deriving from biomolecular interactions. To achieve the excitation of PSPRs, when the light interacts with the metal surface, certain conditions must be satisfied, such as polarization, angle, and wavelength, and the most traditional way to obtain an efficient light coupling is to employ a prism-based scheme (i.e., the Kretschmann configuration), even though other approaches are used, such as diffraction grating and waveguide coupling [10]. For small nanostructures such as metal nanoparticles, boundary and surface effects become important, so that the interaction with the light results in non-propagating collective oscillations of the particle conduction electrons, named localized surface plasmon resonance (LSPR). When light interacts with a metal nanoparticle, electrical charges are accumulated on its surface, thus originating a dipole: the Coulomb attraction between positive and negative charges results in the restoration of forces displacing the electron cloud from the nuclei, with electrical charges starting to oscillate collectively with a unique frequency localized in the UV-visible NIR region of the spectrum [11]. The position, number and width of such modes are determined by several parameters such as particle size, shape, medium refractive index, surface charge, and interparticle interactions, but also from other additional factors such as surface modification (including the deposition of shells, either of another metal, a semiconductor or a dielectric) and composition (doping, alloying) [12]. In addition, the electromagnetic fields localized close to the particle surface are largely enhanced, with the

enhancement being greater near the surface and quickly decreasing for larger distances. In addition, at the LSPR frequency, the scattering and absorption cross-sections are all strongly enhanced [13], thus resulting in great interest in sensing techniques such as colorimetric detection or SERS analysis. In fact, LSPR is the source of the brilliant and intense colours displayed from plasmonic metal nanoparticles and have attracted attention since the Lycurgus cup [14], and recently have been exploited with a growing interest in colorimetric detection. In colorimetric analysis, the event of detection is converted into a colour change, so it is characterized by simplicity, low cost, practicality and the lack of the requirement for bulky and sophisticated instruments because the colour change is revealed by the naked eye. Its intrinsic advantages make it appealing to integrate colorimetric assays into POC devices, and the development of new materials along with new colorimetric strategies has focused enormous efforts in recent years [15].

### 3. Microfluidics Technologies

Aiming to integrate nanoplasmonic biosensors into a POC device, the design of the microfluidic and the optical components is crucial. Microfluidic technologies are exploited in order to create POC devices enabling analysis with samples of a very small volume. The devices produced with microfluidic technologies contain channels and chambers with size dimensions of the order of millimeters, so that fluid flow is laminar (namely, without chaotic turbulence), thus controlling the transport and mixing of molecules, thus resulting in a more accurate and sensitive detection [16]. In addition, with microfluidic technologies it is possible to automatically realize the mixing of the sample with the reagent, the washing, and the cleaning and facilitating sensing. Between the devices adopting microfluidics technologies, the one based on capillary flow, the lateral flow assays (LFA), are the most broadly diffused and commercially popular POC tests (such as, for example, the pregnancy test and glucose test kit) and meet the ASSURED criteria. They are self-operating tools consisting of a strip including a sample pad, a conjugate pad, a nitrocellulose (NC) membrane and an adsorbent pad. These components are combined onto an adhesive backing card in such a way that they are sequentially overlapped [17]. After being introduced onto the sample pad, the sample solution will flow to the downstream components by means of the capillarity, thus performing the test. The next component of the LF strip, the conjugation pad, has been loaded with the micro/nanoparticle coupled to the bio-recognition elements (conjugate): the conjugates will be retained in the conjugation pad during the whole shelf-life of the product, and the analytes will be released from the pad to the NC membrane. In the NC membrane, the analyte molecules migrate until encountering their matching capture components in the test line (T line), where they are immobilized so that a detectable output signal is generated and measured for the analysis. Finally, the analytes that have not been immobilized in the T line are adsorbed in the control line (C line) and the absorbent pad collects the final sample solution, providing the capillary driving force (Figure 1).

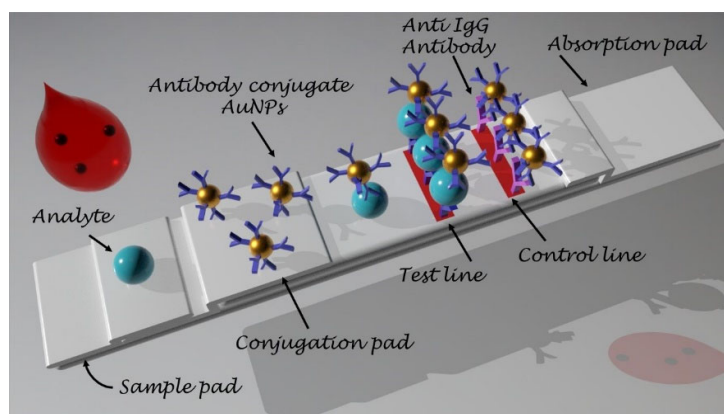


**Figure 1.** Schematic of an LFA strip test.

Generally, the conventional microfluidics devices contain channels created by etching or molding into PDMS, silicone or glass substrates, or other polymers or plastics [18]; however, diagnostics devices can also be produced by patterned paper, obtaining the so-called microfluidic paper-based analytical devices ( $\mu$ PADs). In  $\mu$ PADs systems, sheets of paper are patterned into hydrophilic channels bounded by hydrophobic barriers. Using  $\mu$ PADs systems, the process of the analysis is facilitated by the microchannels patterned on paper substrates: the samples and buffer solutions that must be analysed can flow naturally within the microchannels as a result of the natural hydrophilicity of paper fibers, so that external driving sources are not required. The production of  $\mu$ PADs devices is based on technologies that employ chemical modification or physical deposition techniques to change the material properties of the cellulose matrix [19]. The most conventional methods to manufacture  $\mu$ PADs include wax printing, photolithography, inkjet printing, laser cutting, polydimethylsiloxane (PDMS) stamping and printing, thermal embossing, hydrophobic silylation, and paper folding. The  $\mu$ PADs systems combine the advantages of paper—such as the low cost, the biocompatibility, the low weight and the removal of the need for external support equipment such as pumps or power because the movement of the fluid is controlled mainly by capillary forces and evaporation—with that of microfluidics analysis—such as the requirement of samples of a small volume and the rapidity. In 1949, Muller and Clegg [20] produced, for the first time, paraffin-patterned paper containing microfluidic channels, considered also the first paper-based assay, but it was the work of Whitesides' group at Harvard University [21] which really introduced the  $\mu$ PADs systems to the scientific world. Since then, microfluidic paper-based analysis has experienced a growing interest and an evolution, representing a breakthrough in cost-effective and portable POC diagnostics and a promising alternative to traditional microfluidics devices.

#### 4. Readout Systems

The traditional and most widespread POC devices based on LFA microfluidics are designed for qualitative analysis, providing a binary “positive/negative” answer from the colorimetric signal, but cannot establish the precise concentration of the analyte. For some applications, the simple binary readout is satisfactory, such as, for example, in pregnancy and, recently, in SARS-CoV-2 tests; however, assay quantification is relevant in accurate diagnostics. In some situations, in fact, it is required to monitor the changes in analyte concentration or to take decisions according to the amount of the target analyte, so that quantitative detection is vital. For example, in some complex clinical scenarios, such as cancer, information on the progress/prognosis of the disease and the efficacy of the therapy is provided by changes in analytes. The most traditional method to determine the concentration in a colorimetric test is comparing the acquired signal with a calibration curve produced by the analysis of the sample with a known concentration in an appropriate range, but it is not desirable for POC analysis, so other approaches have been designed. In LFA detection, for example, quantification is performed by readers that have been designed to be portable, user-friendly, and cheap for POC and on-site use. In recent years, apps for smartphones along with readers have been developed for more sophisticated techniques such as SERS. This section will review the recent evolution of signal readers such as smartphone-assisted POC devices and SERS portable readers.

##### 4.1. Smartphone-Assisted POC Devices

To quantify the results obtained from an LFA test, the already-existing and universally accessible technologies are the most valuable in order to design an advanced POC device. Between the plethora of technologies currently available, smartphones have been the subject of a huge evolution, to the point of revolutionizing the daily life of people. Due to their characteristics, such as widespread diffusion, portability, accessibility and sophistication, smartphones are intriguing devices to be included and used as a readout system in POC analysis [22]. The actual smartphones can be considered as a portable miniaturized PC possessing a CPU with high speed, large RAM (random access memory) and sophisticated

camera lenses with Wi-Fi/Bluetooth connectivity, thus fulfilling the requirement for a POC device. Smartphones support sensing transducers in two ways: they are employed as (i) a detector to interpret the changes resulting from the biochemical event and (ii) a data analytics platform to create a database, thus facilitating the eHealth. Smartphone POC diagnostic platforms have been advanced through the design and development of customized Android applications and the integration of optoelectronics, thus ensuring an instrumental interface for the colorimetric, electrochemical, and fluorimetric detection of an analyte in various body fluids, such as blood and saliva. Typically, when integrated into a POC device, smartphones are used for the determination of (i) colorimetric and fluorimetric variations where Android applications and smartphone cameras are employed for colour and imaging analysis and (ii) electrochemical changes by means of a smartphone camera and CMOS detector to interpret and communicate data. Generally, for quantitative detection in colorimetric analysis with a POC device, an algorithm (usually run by an app installed onto a smartphone) is utilized to convert the colour and its intensity in the concentration of the analyte, and the app which processed and interpreted the image is able to communicate the data using cloud systems and wireless technology. As an example, by adding small field-portable fluorescence microscopy accessories to a smartphone, it has been possible to image individual fluorescent nanoparticles and viruses with a diameter down to 100 nm [23], or by incorporating commercially available lens systems, it is possible to image cells, bacteria and biological tissue at 350 $\times$  magnification [24]. In the work of Liedberg [25], a portable smartphone spectrometer to monitor optical changes in real time was developed and applied as an LSPR biosensor by designing an assay for cardiac human troponin (troponin I), the heart-disease biomarker, exploiting AuNPs. Motivated by the outstanding properties of hybrid systems and aiming for their future exploitation for POC devices, Fantoni et al. [26] performed a simulation study showing that LSPR colour filters can be exploited in a low-cost reading set-up. During an early phase, the simulation of the light transmission properties of a transparent substrate decorated with bare and 2D nanomaterial hybridized AuNPs was performed and, following this, the collected results were translated into a lab with XYZ and RGB colour spaces. A quantification of how much and in which manner the process of colour recognition can be affected by several parameters such as particle size and distribution or type of 2D nanomaterial was identified in this stage, so that in a further step, the digital camera of a smartphone along with a colour-recognition algorithm can be exploited as a low-cost reading set up. In this scenario, it is easy to figure out how a smartphone camera, along with innovative output systems based on a smartphone, would be one of the best tools to implement the use of sensing platforms comprising hybrids between plasmonic metal nanoparticles and 2D nanomaterials in point-of-care devices. The breakthrough in colorimetric sensing resulting from the excellent properties of the hybrid compound along with the progresses in microfluidic and optical systems provide a great benefit for the use of next-generation diagnostic tools in real-world applications such as the detection of acute kidney disease (AKI) or the surface spike protein of SARS-CoV-2.

#### 4.2. Surface Enhanced Raman Spectroscopy (SERS)

Raman spectroscopy uses scattered light to identify the vibrational modes of a molecule, thus providing structural information as well as identification through the unique molecular “fingerprint”. The information in Raman spectroscopy is acquired through the Raman scattering of the incident light. As a result of the interaction, the energy of the photon is transferred to the molecule, leaving it in a higher energy state and inducing the polarization of the molecular electronic cloud; then, the photon is re-emitted almost instantly as scattered light [27]. In the majority of scattering events, the molecule energy remains unchanged after the interaction with the light so that the wavelength of the scattered photon is identical to that of the incident photon, and this is classified as elastic or Rayleigh scattering and it is the dominant process. In a much rarer event, the inelastic scattering process takes place, known as Raman scattering, where there is an energy transfer between the molecule and

the scattered photon: in cases where the molecule relaxes to a lower vibrational level thus losing energy, the scattered photon gains the corresponding energy so that its wavelength is blue-shifted (anti-Stokes scattering). Differently, in cases where molecule is excited to a higher vibrational level, the photon loses the corresponding energy and its wavelength is red-shifted (Stokes scattering). On this basis, the Raman shift is a transition induced by the light between the ground state and an excited vibrational molecular state. The main drawback of Raman spectroscopy is to obtain signals with satisfying intensities, caused by the very low number of inelastic scattering events; however, since the unexpected discovery that a Raman scattering boost (which considerably improves the signal intensity) takes place when a molecule is located near a rough metal surface or metal nanoparticles by Fleischmann during measurements of the Raman scattering of pyridine on rough silver electrodes [28], enormous attention has been paid to the phenomenon; therefore, a new Raman spectroscopy, surface-enhanced Raman spectroscopy (SERS), has emerged as a powerful technique for sensitive, fast and accurate analysis, which have benefitted from huge advancements [29] and advancements in new materials such as hybrid compounds between plasmonic metal nanoparticles and bidimensional materials such as, for example, graphene and its derivatives [30].

## 5. Surface Functionalization

The bioactive area, the place where analytes are recognized by specific receptors, is one of the critical components of a sensor, affecting the signal and, as consequence, the limit of detection, the sensitivity, and the overall performance of the device. In light of its importance, when producing a biosensor, one of the most challenging steps is the conjugation of the sensor's active surface with the biological receptors in order to maximize the signal that is proportional to (i) the percentage of the surface occupied by the capturing elements (coating of the bioactive area); (ii) the effectiveness of the binding event; and (iii) the selectivity between the inert area and the bioactive area [31]. In these circumstances, during the design and development of a biosensor, several details must be considered, particularly the capacity of retaining the native conformation of the biorecognition element after immobilization, so that its natural activity is preserved, along with the facility to access the analyte molecules and prevention of non-specific absorption onto the solid substrate. In addition, in the case of a plasmonic sensor, a relevant detail to be considered is the decay length, the distance to the metal surface, which can be decreased exponentially [32], so that the maximum signal is reached when the molecules are attached directly to the particle surface. From this perspective, it is important to immobilize the receptors in such a way that the binding event takes place relatively close to the plasmonic surface, thus ensuring the signal readout. As a consequence of the rapid decay length, furthermore, at low concentrations, the detection of analytes could be challenging because a molecule will scarcely adsorb or be in the immediate surroundings of the plasmonic surface. One of the central points at the time of immobilizing a biomolecule onto a sensor surface is to achieve its proper orientation, namely, the appropriate exposure of the binding sites to the sample where analytes must be detected, because the effectiveness of recognition is stronger, and, also, the orientation affects the density of the receptors on the surface, thus assuring a higher recognition specificity and an improved sensitivity of the sensor. Along with the orientation, optimal immobilization also takes into account stability and activity while performing the analysis, the packing density and the exclusive binding onto the sensing area. Over recent years, several strategies have been developed to immobilize receptors on the sensor surface and, broadly speaking, they can be divided into two main categories: non-covalent and covalent immobilization [33]. The non-covalent immobilization is based on the absorption of biomolecules by means of forces, such as Van-der-Waals forces, hydrophobic interactions and electrostatic or ionic bonds; however, despite the simplicity of the approach, it is not advisable because the control over the biomolecule orientation is limited, resulting in the low performance of the sensing device. Covalent immobilization includes the modification of the surface to integrate reactive groups such as hydroxy, thiol, carboxy, or amino groups

which will then be exploited to attach the bioreceptors. This approach typically requires two steps: (a) the formation of an appropriate self-assembled monolayer (SAM) of bifunctional alkane thiols onto the metal surface operating as a linker and (b) the following cross-linking between the functional thiols and the complementary functional group on the analyte molecule. The choice of the thiol group (-SH) is the most widespread in the case of gold surfaces: the -SH groups strongly attach to the gold surface, thus spontaneously forming an SAM, also exploiting the electrostatic and hydrophobic interactions between the carbon chains. Other approaches are based on the interaction between a biomolecule, acting as a linker, and a second molecule employed for the detection of the analyte, enabling a highly specific and powerful recognition mechanism (bioaffinity interactions). The most popular example of a bioaffinity-mediated immobilization technique utilizes the streptavidin–biotin complex: in this case, streptavidin is immobilized onto the substrate, whereas a biotinylated moiety is attached to the receptor molecule. Despite the further steps required for the chemical modification of the receptor with biotin and to attach streptavidin, this approach provides a highly oriented and stable layer with improved specificity. Another approach is based on the bioaffinity interactions among antibodies and protein A or G produced in bacteria: such proteins are able to selectively bind the Fc portions of Abs, thus assuring the correct orientation and resulting in the proper orientation onto the metal surface, thus guaranteeing high recognition of antigens as well as high purity and long-term stability. In addition, a further approach employs the DNA-directed recognition by means of a single stranded DNA (ss-DNA) able to selectively bind an antibody. Other strategies for the immobilization of receptors have emerged with the progresses in molecular chemistry and bioengineering, such as calixarenes, DNA-mediated coupling, or recombinant antibody fragments; however, they are less frequently utilized. Many biological systems showing an exceptional affinity and specificity towards their corresponding analyte molecules have been employed to develop sensing devices [34]. As an example, aptamers (RNA oligonucleotide sequences or single-stranded DNA (ss-DNA) with the ability to bind, in a specific manner, an analyte possessing an affinity comparable to that of antibodies) are frequently used as receptors, but their production is labour-intensive and time-consuming, although their engineering is easier and more suitable compared to that of antibodies [35]. Sugars are less commonly used, but sometimes could be very selective, but they need to be modified before being anchored to the surface. Recently, molecularly imprinted polymers (MIPs) are emerging as recognition elements: they are affinity polymers provided with specific binding sites designed with the proper shape, size and orientation of the functional groups for the selective trapping of the target molecule, offering an interesting alternative for their affordability and robustness [36]. Antibodies, or immunoglobulins (Abs), are the biological recognition elements most frequently used in the development of a biosensor: they are large glycoproteins of about 150 kDa which are part of the immunoglobulin (Ig) superfamily produced by the immune system to recognize external antigens in order to neutralize them and induce an additional immune response [37,38]. The bone structure of an antibody includes two identical light chains and two heavy chains connected through disulfide bonds in the hinge region to form a complex quaternary Y-shaped structure [39]. The light chains are formed by two identical light domains: a constant domain ( $C_L$ ) and a variable domain ( $V_L$ ). In contrast, according to the type of heavy chain, antibodies can be classified into five distinct classes—IgA, IgD, IgE, IgG, and IgM—which are different in structure and function. IgA, IgD and IgG have three constant domains ( $C_H$ ) and one variable ( $V_H$ ), whereas the IgE and IgM have four constant domains and one variable [40]. The whole quaternary structure of the antibody can be divided into three fragments: the first two, recognized as Fab portions, are responsible for the antigen recognition and are localized at each tip of the Y (corresponding to the “horns” of the antibody) and contain one light chain, one variable heavy domain and one constant heavy domain ( $V_L$ ,  $C_L$ ,  $V_H$  and  $C_H$ ) [41]. The remaining fragment is the fragment crystallizable region ( $F_C$ ) and is located at the base of the Y structure: it comprises the rest of both heavy chains and is responsible for the interactions between the antibody and other members of the immune

system [42]. Finally, the smallest fragment of an antibody functioning in antigen-binding activities is the single-chain fragment variable (scFv) which is composed of the variable regions of the light chain ( $V_L$ ) and heavy chain ( $V_H$ ) linked by a flexible peptide to generate a single-chain protein with an affinity for its antigen comparable to that of the parental mAb [43] (Figure 2).

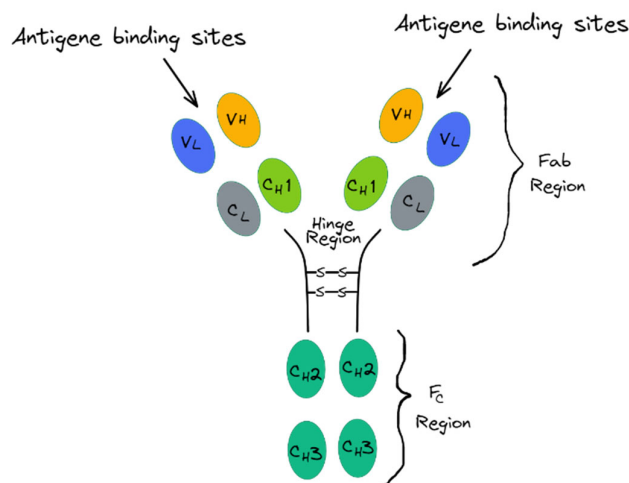


**Figure 2.** Illustration of antibody structure: C indicates the constant domain and V the variable domain; H denotes the heavy chain and L the light chain; S-S is the disulfide bond; Fab is the fragment antigen-binding domain and Fc the fragment crystallizable domain.

Immunoassays are based on the specific antigen–antibody interactions and the detectable signal produced by the changes in a substrate to qualitatively and quantitatively determine molecules: compared to standard instrumental analysis, they offer several advantages such as low cost, simple pre-treatment with no need for trained professionals nor complex equipment, rapid response and, more significantly, they have high sensitivity and specificity, thus offering great potential as a POC device. There are several formats for immunoassays, including the most famous, enzyme-linked immunosorbent assay (ELISA), chemiluminescent immunoassay (CLIA), quantum dot fluorescence immunoassay, colloidal gold immunoassay, microarray-based immunoassay and many others; however, all of them rely on the specific binding between the antibody recognition sites and antigenic determinants. Within that framework, it is extremely important to design specific antibodies with a high affinity for the analytes, to improve the specificity. In standard immunoassays, polyclonal and monoclonal antibodies are usually exploited, but in recent years, a new type of antibody, recognized as “nanobodies,” is emerging as an appealing alternative to conventional antibodies and ideal basic components for a broad assortment of sensing devices and tests to be used in medical, biotechnological, and environmental fields [44]. Nearly 30 years ago, in 1993, heavy-chain antibodies (HCAbs), naturally lacking light chains, were casually discovered in the peripheral blood of *Camelus dromedarius* by the Belgian immunologist Hamers and his colleagues, paving the way for a new type of antibody, the nanobodies. A heavy-chain-only antibody consists of two heavy-chain constant regions (CH2 and CH3) while lacking the first constant CH1 domain, a hinge region, and a heavy-chain variable domain (VHH), preserving the antigen-binding capacity of the antibody [45]. The molecular mass of the HCAbs is about 95 kDa while their variable antigen-binding domains (VHH) have a molecular mass of 12–14 kDa with a prolate shape with dimensions of 4 nm × 2.5 nm × 3 nm (Figure 3)

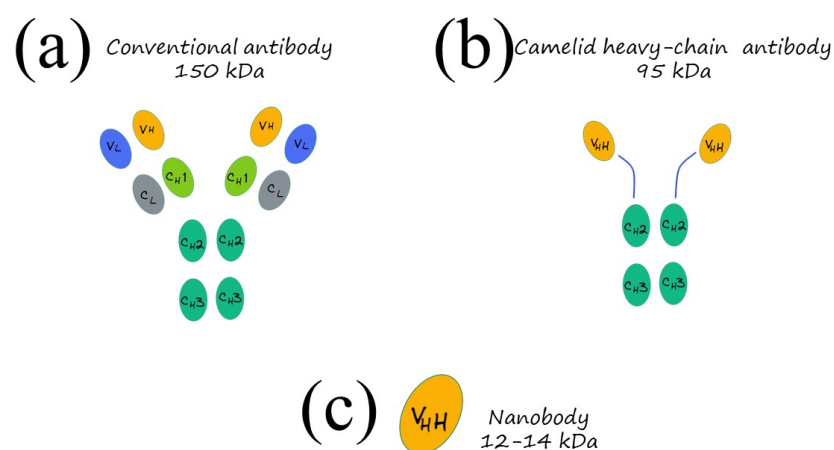


**Figure 3.** Graphical representation of the different types of antibody structure: (a) a classical antibody with heavy and light chains; (b) a camelid antibody consisting solely of two identical heavy chains; (c) the antigen-binding region consisting of a single variable domain VHH or nanobody.

In the VHH domain is included the strong affinity towards its related antigen and the full potential to bind the antigen, so it is considered the smallest naturally occurring fragment with intact antigen-binding activity. The small size, in the low nanometre range, was the stimulus for introducing, in 2003, the term “nanobody” as a trademark of the company Ablynx, which has subsequently been utilised as a general tag for those proteins. They are distinguished by superior properties, compared to conventional antibodies—such as, for example, elevated stability—expressed in various forms: tolerance to increased temperatures; prolonged shelf life; resistance to several harsh conditions, such as exposure to different pH values from physiological, elevated pressure; proteolytic degradation; and the fact that chemical denaturants hardly affect their antigen-binding ability. The efficient ability to refold after thermal, physical and chemical denaturation is the basis of the nanobodies’ robustness. Within the framework region 2 in nanobodies, named FR2, four hydrophobic and highly conserved amino acids are replaced by smaller and/or more hydrophilic amino acids, thus increasing solubility in aqueous solutions. The simple monomeric structure and the lack of post-translational changes make it possible to express nanobodies in milligram quantities per litre of culture in shake flasks by means of microbial expression systems such as *Escherichia coli*, *Saccharomyces cerevisiae* and *Pichia pastoris*, thus enabling industrial mass production at a low cost and the availability of purified antibodies with homogeneous properties in sufficient amounts [46]. In addition, nanobodies possess an improved ability to identify antigens compared to conventional antibodies arising from their unique structure and small size, which make it possible to bind sites that are difficult to reach by conventional antibodies [38]. As a result of their extraordinary properties, nanobodies, in recent years, have emerged as a powerful tool to design and develop next-generation immunoassays. The interest in the use of nanobodies to develop sensing platforms is only in its early stage, so much still needs to be explored in this field. In the work of Simões [47], an effective and simple strategy for the spontaneous self-assembly of nanobodies on gold surfaces was proposed, which has remarkable potential to be employed to develop sensing platforms. Firstly, the model nanobody NbVCAM1, targeting the vascular cell adhesion molecule-1 (VCAM1), was strategically engineered at its C-terminal, at the opposite end of the binding antigen pocket, with an alkyne-modified cysteine with the capacity to absorb on gold surfaces. As a result of the incorporation of the modified cysteine, nanobodies can be directly immobilized on gold sensors, forming a monolayer that was then investigated using many complementary surface-analysis techniques such as three-dimensional (3D) Orbitrap secondary ion mass spectrometry (3D OrbiSIMS), time-of-flight secondary ion mass spectrometry (ToF-SIMS) and circular dichroism (CD). The obtained results indicated that the activity and structure of nanobodies are maintained upon the immobilization and confirmed the arrangement in a stable, homogeneous and well-packed monolayer onto

the gold surface. In addition, experimental and theoretical results confirmed the high proportion of well-oriented nanobodies led to a strong ability to bind antigens, thus paving the way for the design and development of robust, reliable and stable sensing platforms for the sensing of biomolecules. While nanobodies (Nbs) technology and the immune-sensing area are currently undergoing considerable progress, the functionalization of AuNPs with Nbs is still in its early phase; thus, aiming to take further steps forward in this direction, Goossens [48] elaborated a strategy to obtain stable AuNPs functionalized with nanobodies (Nb-AuNP). Using three different types of well-characterized nanobodies (BCII10 binding  $\beta$ -lactamase II of *Bacillus cereus*, cAbLys3 able to identify the hen-egg white lysozyme and a GFP binder), the practicability of functionalised AuNPs with Nbs through physical absorption, along with the possibility of applying the rules of antibodies absorption to gain further insights into the mechanism for the production of stable Nb-AuNP, were investigated. When developing a sensing system, colloidal stability is a key point as well as the functionality of the biological molecules. In the case of monoclonal antibodies (mAbs), the larger size enables the formation of repulsive barriers between particles by means of electrostatic hindrance; however, due to their reduced size, in the case of Nbs, the driving repulsive force is their charge. The absorption of antibodies produces stable particle complexes only when the negative charge of Nbs is negative and the values of the solution ionic strength are low. In such circumstances, no unfolding mechanism occurs at the interface with gold, so that the produced Nb colloids are functional units with great potential to be employed in immune assays. On this basis, engineering Nbs in such a way as to realize an optimal electrostatic configuration by integrating strong binding residues, such as cysteine, and then creating Nb-AuNP colloids through physical absorption has been proposed as a general strategy for the development of a successful sensing system. One of the early approaches in the use of AuNPs conjugated with nanobodies as a sensing device was presented in the work of Alsadig [49]: an advanced biosensing platform was created through a combination of a mixed self-assembled monolayer (SAM) of thiolated single-stranded DNA (ssDNA) and bio-repellent molecules, indicated as top-terminated oligo-ethylene glycol (TOEG6) and the DNA-directed immobilization (DDI) of DNA–protein conjugates. One of the primary challenges related to the immobilization of protein onto a solid substrate concerns the preservation of the protein functionality by preventing alterations in their structure during the immobilization progress, along with the steric hindrance of the recognition sites. In that direction, the DNA-directed immobilization (DDI) of DNA-conjugated proteins, resulting from the combination of short ss-DNA oligos self-assembling with the sequence-specific hybridization of complementary DNA strands conjugated with definite proteins and/or proteins binders, emerges as a versatile tool to transform a DNA microarray into a protein microarray exploiting Watson–Crick hybridization while retaining the protein structure. Unlike covalent binding, when biomolecules are anchored by means of DDI onto a surface, they completely preserve their functionality, as well as the steric hindrance being reduced by employing DNA strands as spacers between the substrate and the biomolecules of interest, thus resulting in a broader opportunity for molecular recognition. In light of implementing the DDI approach to create sensing platforms, AuNPs were functionalized with an optimized quantity of ssDNA molecules in order to prevent the effects of steric hindrance and to ensure the active loading of the DNA–protein conjugates. To avoid the absence of the specific binding of protein or small molecules, the thiolated ssDNA moieties were mixed with bio-repelling TOEG6 molecules (ss-DNA/TOEG6@AuNPs). In a successive step, the potential of the ssDNA-modified AuNPs in the context of cancer-associated antigen sensing was investigated employing the complementary ssDNA fragments conjugated with the C8 nanobody fragment optimized for the recognition of a specific biomarker extracellular domain of the human epidermal growth factor receptor 2 (HER2-ECD), a transmembrane protein belonging to the family of the epidermal growth factor receptors (EGFRs) and overexpressed in 15–30% of breast-cancer patients. To detect the hybridization of the ss-DNA/TOEG6@AuNPs with the C8-labelled DNA target, the changes in the refractive index, induced by the biorecognition event occurring close to the AuNPs' surface,

were evaluated by means of a novel technique. Employing a conventional LSPR detection technique, the sensitivity is too low to identify the binding of ECD-HER2 to the functional nanoparticles, so that, to assure the enhanced sensitivity of the test, an approach based on a miniaturized gel electrophoresis chip integrated with online thermal lens spectroscopy (MGEC-TLS) was employed as a sensing system, thus obtaining a sensitivity 100-fold higher than the standard SPR resulting from the acquisition of quantitative information through the relation of the immunocomplex biological identification with the mobility of the particle. The time required by the conjugates to arrive at the measurement point was measured and, as expected, increases with the quantity of HER2-ECD, thus making it possible to relate the concentration of loaded HER2-ECD to the time of MGEC-TLS signal, namely, the signal registered when the sample passes through the measurement point. The changes in the refractive index were amplified by the presence of the gel matrix and are associated with the temperature alterations generated by the energy-to-heat conversion of light adsorption at the LSPR wavelength, thus obtaining a system with enhanced sensitivity combined with ease of preparation and reduced costs, with potential to be used in contexts of low or limited resources (Figure 4).

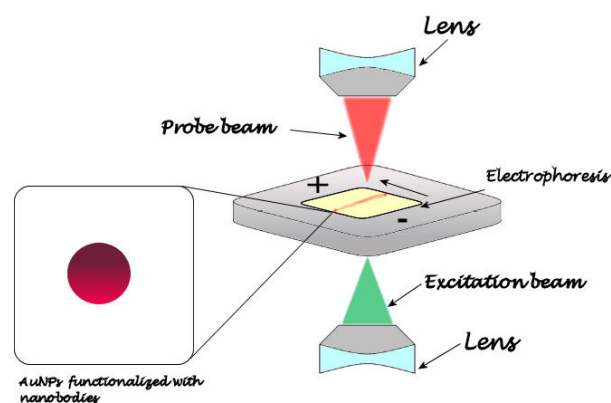


**Figure 4.** Schematics of miniaturized gel electrophoresis chip (MGEC) integrated with online thermal lens (TL), approach used in ref. [49].

A colorimetric and photothermal dual-mode immunochromatographic test strip (KNb-DITS) based on the determination of nanobodies for *Salmonella Typhimurium* (*S. Typhimurium*) was presented in the work of Zhang [50], which provides an innovative path and ideas for foodborne pathogen detection and, more broadly, for immunosensing POC devices. Encouraged by their intrinsic advantages, nanobodies were integrated in colorimetric/photothermal sensing probes. Firstly, flower-like three-dimensional (3D)  $K_{0.27}MnO_2 \cdot 0.54 H_2O$  (KMO nanoflowers) were synthesized using hydrothermal methods and then decorated with AuNPs; successively, the KMO@Au composites were effectively conjugated with anti-*S. Typhimurium* Nb9 was used to form the colorimetric/photothermal-KMO@Au@Nb9 sensing probes. As in classical tests, the strip is composed of a sample pad, nitrocellulose (NC) membrane, absorbent pad, and PVC backing. The test line (TL) and the control line (CL) are placed onto the NC membrane and are made up of capture anti-*S. Typhimurium* pAb and anti-HA tag mAb. In the presence of the target analyte *S. Typhimurium*, an interaction with the capture anti-*S. Typhimurium* pAb of the TL is established, so that a KMO@Au@Nb9-*S. Typhimurium* complex is formed, which can be directly observed by the naked eye and the colour analysed using software. In addition, *S. Typhimurium* can be detected in a photothermal mode: the TL line is irradiated with a laser of 808 nm (radiation in the NIR region of the spectrum) and temperature and images collected by means of a portable infrared camera and processed for a quantitative analysis. Using the KNb-DITS sensor, it is possible to easily perform not only visual qualitative detection with the naked eye, but also quantitative detection using both colorimetric and photothermal analysis. The colorimetric detection is able to detect the *S. Typhimurium* with a LOD of  $10^4$  CFU mL<sup>-1</sup>,

whereas in photothermal mode the obtained LOD is  $10^3$  CFU mL<sup>-1</sup>, thus providing a new direction for advanced POC devices.

## 6. Multiplexed Analysis

The detection of different analytes at the same time enables the performance of accurate diagnostics about the health of an individual, so that personalised therapy could be designed, which also offers the additional advantages of lowering the analysis costs and significantly simplifying the diagnostic workflow [51]. The benefits arising from the analysis performed in a single run make the multiplexed detection an intriguing alternative to other approaches. Despite the promising advantage of supporting future advances in personalized medicine, multiplexed detection still presents some challenges, making its full implementation in real diagnostics difficult [52]. One of the main issues is to generate a sufficient number of signals that are each distinguishable from the other by means of the detection instrument in order to distinguish the individual analytes. This means that when the signals can be more easily distinguishable and their total number is greater, better detection could be obtained. Within a biological sample, the concentrations of analytes may differ by an order of magnitude, such that the additional need concerning the linear range and the detection sensitivity is introduced. In addition, it is necessary to reduce the time and the costs of the analysis, as well as to minimize errors resulting from the complexity of the operations, so it is critical to simplify the overall detection process as much as possible. In light of effective clinical implementation, several strategies have been designed to face the challenges arising in multiplexed detection, along with different approaches to analysis. During recent years, plasmonic nanoparticles have attracted increasing interest for their unique properties; they have proven to be a promising resource in the multiplexed detection of analytes [53]. In fact, by means of different synthetic techniques [54], researchers are able to control various parameters such as size, shape, composition, surface modification, surface charge and so on; it is possible to produce the desired optical response such as position and shape of the LSPR peak in the UV-visible spectrum. Given the possibility of synthesizing plasmonic nanoparticles with tailored optical properties, it is easy to figure out how including various nanoparticles generating different signals in a unique assay enables the detection of multiple analytes in a single run. On these bases, several approaches have been designed to exploit plasmonic metal nanoparticles in multiplexed detection. Spectroscopic methods are emerging as analytical techniques for the multiplexed detection of analytes, due to their remarkable advantages, such as ultrasensitive detection down to the level of the single molecule and the ability to perform the measurements in a biological environment without the need for preparing the sample in advance. Despite this great potential, there are still some limitations that must be overcome to effectively implement SERS technology in multiplexed analysis for daily medical diagnostics. One of the main difficulties is the number of the analytes that can be detected simultaneously in a multiplexed analysis: when increasing the number of molecules to be revealed, competing signals are likely to arise, so that the vibrational modes of different molecules are likely to overlap, thus making the interpretation of the spectra difficult if not nearly impossible. A way to solve the complexity of the SERS spectra of multiple analytes is to apply chemometric algorithms, such as principal component analysis (PCA), partial least-squares regression (PLS) and hierarchical cluster analysis (HCA) [55]. The multiplexed detection of analytes could be performed in one of two modalities: the first is the direct one involving the use of nanoparticles with bare surfaces to obtain enhanced Raman signals, whereas the second is the indirect modality, where SERS tags provide the signal and confirm only indirectly the presence of the analyte. The elevated quantity of salt, the low analyte concentration, typical of the physiological environment, and voiding of results in the nanoparticle aggregation make the reproducibility and quantitative identification of the target limited, and, in this context, indirect detection becomes increasingly important along with the concept of the SERS tag (also called encoded SERS nanoparticles) [56]. A SERS tag is a probe created to recognize, in a selective way, the target molecule by means of the targeting moieties de-

signed with high specificity towards the analyte molecules (such as, for example, antibody, polymers or antibodies) and to generate the SERS signal. Even though the characteristics strongly rely on the specific applications for which the tag has been designed, the SERS tags share some common characteristics: (a) the presence of a plasmonic core generating the electromagnetic field required for the enhancement of the Raman signal; (b) the addition of a Raman reporter molecule (SERS code) which originates the unique molecular fingerprint arising from the encoded particle; and (c) a protecting layer to stabilize the nanoparticle against aggregation and to provide improved biocompatibility to the particle surface [57]. In Figure 5, a schematic of a SERS nanotag is depicted.

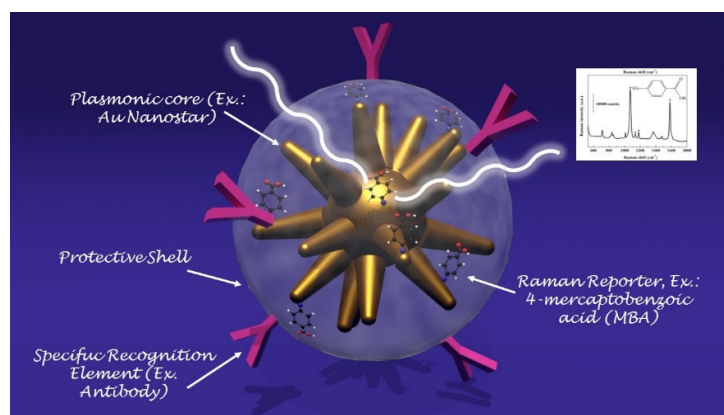


**Figure 5.** Schematic representing a SERS nanotag's main components.

On this basis, it can be easily figured out how multiplexed assays can be produced by designing different SERS nanotags generating different signals and successively integrating them in a unique test. The production of SERS nanotags originating non-overlapping signals is an effective strategy for the multiplex detection of analytes so that their integration into advanced POC devices is beneficial to the rapid determination of biomarkers in complex fluids such as blood or saliva. The optical properties of plasmonic metal nanoparticles have also been exploited to perform multiplexed analysis in other multiplexed technologies: for example, when designing LFA devices, the most straightforward and direct method to realize multiplexed detection is creating an array of parallel test lines (TLs) on the detection zone, where every single TL is responsible for the identification of a different analyte. The majority of analyses adopting this kind of multiplexed detection are able to determine up to three analytes [58]. One of the critical drawbacks with multiplexed analysis with LFA devices is the reduced length of the detection zone, limiting the number of TLs that can be included in the assay. To insert more TLs, the test strip should be extended, which exponentially increases the assay time. Alternatively, the detection of different analytes within a single TL, as long as it maintains simplicity in the production and in the results read out, could be performed by designing a single test line with two or more different bioreceptors conjugating the analytes. When using a single TL to perform a multiplexed analysis, various labels generating signals that can be easily distinguished, such as, for example, different plasmonic nanoparticles, must be designed and exploited. In view of taking better advantage of the test area provided by lateral flow strips, TLs have been replaced with microfluidic arrays, where a microarray is an ordered arrangement of various assay units into a single device [59].

## 7. Applications

### 7.1. Smartphone-Assisted Devices

In the work of Choi [60], a smartphone-assisted point-of-care (POC) bioassay to detect urea for the daily monitoring of renal and hepatic dysfunction diseases was developed. At the basis of the sensing system, there is the colorimetric detection of urea relying on the production of silver nanoparticles (AgNPs) integrated with an image-analysis system

by means of a smartphone. Through urease, urea is hydrolyzed in  $\text{NH}_3$  and  $\text{CO}_2$ , thus activating tannic acid, which is sensitive to pH, and reducing  $\text{Ag}^+$  ions into AgNPs. Due to their LSPR, AgNPs display a yellow colour: the quality of the colour, associated with the LSPR position and intensity, depends on the number of particles generated. To facilitate the readout of the signal, a paper sheet was exploited as the substrate: using a laser printer, circular hydrophobic black zones were printed around hydrophilic sampling areas. The hydrophilic area inside the black hydrophobic circles was then loaded with urease; in a successive step, solutions at different concentrations of urea were added to the areas of the paper strips functionalized with urease. After a few minutes, the sensing solution composed of tannic acid and  $\text{AgNO}_3$  was added and, as a result, the sensing area displayed several colours depending on the urea concentration. In this direction, a rough analysis of the urea concentration is possible with the naked eye, but to obtain more precise information, an analysis assisted by a smartphone was performed. The corrected RGB ratio showed a linear correlation with urea concentration, so that the urea concentration was determined using smartphone software based on that relation, obtaining an LOD of 2168 mM for urea in human urine samples. Stimulated by the need for a fast and reliable test, the *ironPhone* system was developed in the work of Srinivasan [61] as a POC device to quantify human serum-ferritin concentrations, a biomarker for the status of iron. The *ironPhone* system is composed of a lateral flow immunoassay (LFIA) test strip developed specifically for serum ferritin, a test-strip reader and the *ironPhone* app to display the test results after analysis realization. The first part of the sensing device is the LFIA test strip contained in a cartridge and consisting of a polyester backing layer on which a sample, conjugation and absorption pad are deposited along with a nitrocellulose membrane containing the test and the control line. The LFIA test strip was designed to perform a sandwich immunoassay analysis: firstly, a drop of blood from a finger is introduced onto the inlet of the test strip, in the sample pad, followed by the chase buffer, saturating the sample pad and thus initiating the capillary flow needed to transport the elements of the sandwich immunoassay. In the sample pad, the whole blood sample is filtered, so that the serum is separated and it alone is allowed to flow along the conjugation pad. After the filtration, in the conjugation pad, the serum interacts with the AuNP–anti-ferritin conjugates, which are able to bind the ferritin molecules contained in the initial sample. Successively, the AuNP–anti-ferritin conjugates transporting the ferritin molecules flow to the nitrocellulose membrane, which binds to the polyclonal anti-ferritin antibody forming the test line, thus creating a strong colorimetric signal. The AuNP–anti-ferritin conjugates passing through the test line without binding are then captured by the anti-mouse antibody composing the control line, thus displaying a weak colorimetric signal: as the ferritin concentration increases, the colour intensity of the control line decreases; whereas, for lower ferritin levels, the test line shows a weak colour leading to a strong signal in the control line, indicating that the most of the unbound AuNP–anti-ferritin is bound to the secondary antibody of the control line. At this point, the sample flows to the absorbent pad. Once that the test and control line are ready and the sample has run until the absorption pad, the test strip is inserted within the LFIA strip reader, where the colorimetric signals are amplified and captured from a camera and analysed using the *ironPhone* app to obtain information about the ferritin concentration. In 2016, the same group developed the *NutriPhone* system, a system comprising of a test strip, a test-strip reader and a smartphone app, to quantify the levels of Vitamin B12 in the human blood [62]. *NutriPhone* works in the same way of the *ironPhone* system, but, in this case, the AuNP–anti-ferritin conjugates were replaced with AuNP–anti-B12 conjugates and the test and control lines were composed by Vitamin B12-BSA (bovine serum albumin) conjugate and anti-mouse IgG produced in goat (Figure 6).

Motivated by the need for a rapid and reliable diagnosis to counteract the 2014 outbreak of Ebola virus disease (EVD) in West Africa, in the work of Brangel [63], a POC test for Ebola virus detection was designed. In the developed test, the sample is applied onto the sample pad and migrates to the conjugation pad where complexes between the target analytes and antihuman antibody IgG–gold nanoparticle conjugates are formed.

From the conjugation pad, then, the sample runs towards the analytical pad, where the targeted IgG serum antibodies against single or multiple recombinant Ebola viral proteins bind to detection lines, resulting in a visual red-purple line. In addition, a control line is introduced to validate the assay. Two platforms were developed for single detection by means of Sudan virus (SUDV) recombinant glycoprotein GP1–649 or multiple detection using the SUDV recombinant proteins VP40, NP and GP1–649. Over the course of time, five distinct species of the ebolavirus genus have been detected, four of which are etiological agents of the viral haemorrhagic Ebola virus disease (EVD); thus, the sensing platform has been upgraded for viral-subtype identification: in that case, a multiplexed detection line contains the recombinant glycoprotein (GP1–649) for different Ebola viral species such as SUDV, Ebola virus (EBOV) and Bundibugyo virus (BDBV). In addition, the sensing strip is combined with a compatible smartphone application for semi-quantitative detection. After inserting the patient data in the app login window, the analysis window opens: after aligning a red box between the test and control lines, the results are presented. Based on the relative intensity of the test line and on an evaluated cut-off threshold, the app determines if the result is positive or negative. In addition, by means of the app, data storage and sharing is possible, as well as geographical tagging of the tested individuals in Uganda.



**Figure 6.** Nutriphone system overview illustrating the custom vitamin B12 test strip along with the app and the box reader.

### 7.2. Liquid Biopsy

The evaluation of the cancer mutational profile is crucial in cancer therapy, and in routine diagnostics is performed through a fragment of the primary tumour or metastasis; nevertheless, there are some disadvantages to this kind of test. For example, surgical intervention is required to obtain tumoral tissues, thus widely limiting the sampling, or the presence of multiple tumour sites leads to a complication in the cancer characterization. Additionally, the intra-tumour heterogeneity, especially in the case of a single biopsy test, could lead to untrustworthy results [64]. In this context, there is a strong need for analysis requiring non- or minimally invasive procedures through which real-time monitoring of the patient's cancer molecular alterations is possible. Very recently, the analysis of circulating tumour cells (CTCs), taking the name of “liquid biopsy,” has created new avenues for cancer diagnostics, involving improved risk staging and evaluation, and early tumour detection, and, in cancer therapy, the control of tumour evolution as well as the early detection of relapse. Initially, a liquid biopsy was exploited to detect CTCs, cancer cells detached from a primary tumour and/or metastatic lesion(s) and traveling through the bloodstream to other parts of the body; however, now, it has been extended to other components released by the tumour in the body fluids, such as cell-free circulating nucleic acids (DNA, mRNA, and non-coding RNA such as micro-RNA or long non-coding RNA), “tumour-educated platelets” (TEPs) or vesicles such as exosomes [65]. Due to its characteristics, SERS has emerged as a new tool to perform liquid biopsies, with the final objective of developing

fast and cheap diagnostics, and prognostic and predictive tools that can be employed in the point-of-care setting by simply scanning a biofluid sample with a laser [66,67]. A novel lateral flow strip assay for mutational analysis of ctDNA (cell-free circulating tumor DNA) in blood samples for liquid biopsy based on gold nanoparticles was developed in the work of Kalligosfyri [68]. The test strip is composed of an absorbent pad, a nitrocellulose membrane (diagnostic membrane) containing the test zone (TZ) and the control zone (CZ), a conjugate pad and an immersion pad. A plastic surface is used as a support for all the components, and the ends of the pads are overlapped so that the proper capillary flow of the running buffer through the strip is ensured. The CZ contains biotin molecules from b-BSA conjugates, capable of collecting the excess of AuNPs functionalized with streptavidin (SA-AuNPs). This zone guarantees that the lateral flow assay works properly and it must be always visible. The so-developed method involves ctDNA isolation, PCR amplification of the KRAS gene, and a multiplex primer extension (PEXT) reaction, so that the strip for the visual analysis is not yet completely ready as a POC device. Motivated by the significant death rate caused by the scarcity of sensitive analytical devices for the early detection of the disease and the lack of relevant biomarkers relevant to diagnosis, Tadimety et al., in their work [69], designed and developed a nanoplasmonic platform based on Au nanorods for the detection of pancreatic ductal adenocarcinoma, which has great potential for liquid biopsies. One significant biomarker in a liquid biopsy is the circulating tumour DNA (ctDNA) which, due to its very short half life in peripheral blood, is able to give information about genetic and epigenetic alterations occurring in the tumour. Due to a prevalence rate of 88% in pancreatic cancers, the mutations in the KRAS gene were selected as a target: the most common mutations are localized in coding base 35 of exon 2 and, between them, the c.35G > T mutation replacing glycine 12 with a residue of valine (G12V) was selected: due to its prevalence in 37% in pancreatic cancers and from a study [70], this is the most common mutation in the KRAS gene. Once the target of the test is selected, the nanoplasmonic platform is prepared: after activating the surface for the binding of the peptide nucleic acid (PNA) probe through NHS/EDC chemistry, the Au nanorods are later conjugated to the G12V mutation in the KRAS gene. To be specific, the structure of PNA is a hybrid between a nucleic acid and a protein, with the backbone of a protein and functional nitrogenous bases linked through a tertiary acetamide, and in order to realize how the selectivity towards the binding of the mutant over the wild type could be improved by introducing mutations into the peptide nucleic acid probe, a simulation of the DNA hybridization was carried out. From the simulation, a PNA with an additional mutation two base pairs away from the mutation of interest showed the best selectivity between mutant and wild-type capture, so it was selected to functionalize the Au nanorods' surface and the hybridization with the DNA was performed using UV-spectroscopy. As a consequence of hybridization, the LSPR peak in the spectra shifted towards longer wavelengths, linearly depending on ctDNA concentrations, so that, using solutions at different concentrations, it was possible to calculate an LOD of 2 nanograms of ctDNA per milliliter. The sensing transducer was tested in both buffer and spiked healthy-patient serum, assuring a sequence-specific capture of ctDNA and a strategy to improve the selectivity towards the requested point mutations by means of the accurate design of the probe. The high specificity displayed in the results lays the groundwork for realizing multiplexing and arrayed sensor designs by integrating the principles outlined in the work on a chip.

### 7.3. Wearable Plasmonic POC Devices

In light of personalized healthcare, wearable biosensors have attracted growing interest as a new real-time and non-invasive detection technology. To obtain a deep insight into the human body at a more profound molecular level, several kinds of wearable biosensors are based on plasmonic nanoparticles. The work of Mogera [71] describes a wearable plasmonic paper-based microfluidic device for continuous analysis of sweat. Most of the sensing systems exploit enzymes and antibodies, but they tend to degrade over time, thus

undermining their performances and, in order to create a more stable device for continuous measurement, a microfluidic device integrated with plasmonic paper was designed and then tested for the detection of uric acid (UA), a risk biomarker for cardiovascular diseases, kidney diseases, and type-2 diabetes. The sensing device has a layered structure: at the bottom is placed a stretchable medical-grade double-sided adhesive tape, forming a mechanically robust interface between the skin and the adjacent layer of the device. A black carbon double-sided adhesive, blocking laser radiation to avoid skin damage during in-situ SERS analysis, is enclosed between the double-sided adhesive and the adjacent layer, the microfluidic system. In the developed device, the microfluidic system is an effective microfluidic channel made of cellulose chromatography paper with a serpentine design, providing flexibility and stretchability to accommodate skin deformation without altering device performance, which transports the excreted sweat. A large inlet opening is able to enhance the access to sweat glands, thus maximizing the collection of sweat, whereas at the end of the microchannel is localized an outlet to avoid back pressure. The layer above the microfluidic channel is the plasmonic sensor. It consists of plasmonic paper immobilized in different locations along the microfluidic channel and it is the element of the device that quantifies the concentration of analytes in sweat by means of SERS spectroscopy. The plasmonic paper is formed by gold nanorods (AuNRs) synthesized according to a seed-mediated growth protocol adsorbed on a chromatography-grade filter paper and cut into squares of  $2\text{ mm} \times 2\text{ mm}$  or circles with a 1 mm diameter. All the layers are then encapsulated with a polydimethylsiloxane (PDMS) film: it displays well-defined Raman bands serving as a reference to quantify the analytes of interest in the sweat and, in addition, it is optically transparent, it prevents contamination from the environment, and it minimizes the evaporation of sweat. After testing the mechanical properties, the flow characteristics, and the SERS performance of the sensing layer, the device was exploited to detect UA in healthy human subjects. By means of a portable Raman spectrometer with a flexible fibre probe focused on the sensing part of the system, an SERS spectrum of the sweat was collected and the concentration of UA quantified. For this wearable plasmonic paper-based microfluidic device, an LOD of  $1\text{ }\mu\text{M}$  was revealed; however, despite its great potential as a POC device, it needs still some improvements. In fact, the readout is based on a handheld Raman spectrometer, it was not developed as an integrated electronic readout system (Figure 7).

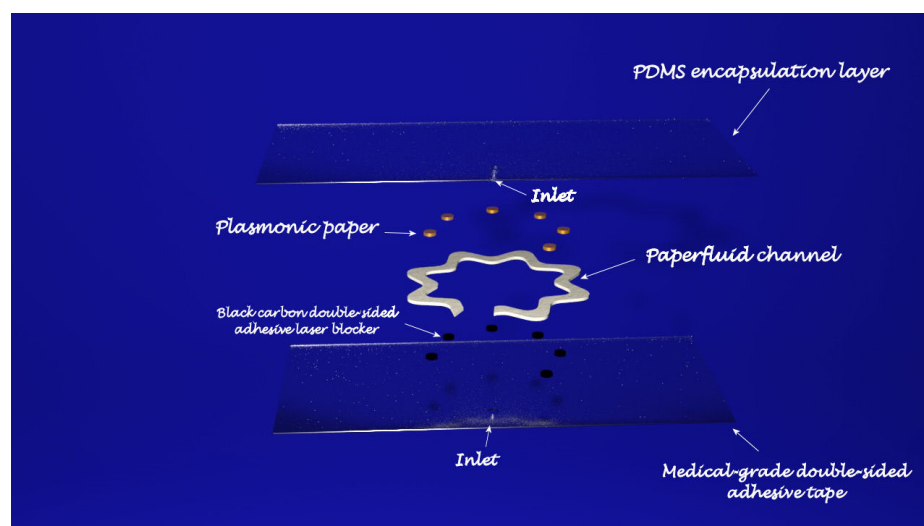


Figure 7. Parts of the wearable POC devices discussed in ref. [71].

In the work of Koh [72], a wearable SERS sensor was developed as a skin-adhesive patch and successively tested to detect 2-fluoromethamphetamine (2-FMA), which is an analogue of methamphetamine. The basement layer is composed of a silk fibroin protein film (SFF): it contains nanopores which were created in the  $\beta$ -sheets domains of the SFF

matrix and are able to filter the molecules. Anyway, the size of the nanopores in the SFF layer can be controlled during the successive process of crystallization, thus allowing a different grade of permeability depending on the nanopore size. A layer of silver nanowires (AgNWs) was then deposited onto the SFF film: inside the layer, the AgNWs form a network with a random structure and at the intersections, hotspots are created with a high density. The SFF/AgNWs were then transferred to an adhesive, transparent dermal patch which protects the wearable sensor from contamination and oxidation when it is worn. In molecular penetration tests, about 90 min are required for the molecules to diffuse through the SFF layer until the AgNWs. Once assembled, the SERS patch was tested for analysis using different water-soluble Raman-reported dyes (4-aminothiophenyl, DAPI, methylene blue, rhodamine B, eosin B, eosin Y and erythrosin B) in order to determine the molecular weight beyond which the SERS performances are reduced; the results showed that the system is well suited for Raman reporters with a molecular weight lower than eosin B. molecules, as higher molecular weights were not filtered by the SFF layer. To evaluate the performances of the wearable SERS patch, 2-FMA was selected. In this case, a solution of 2-FMA was added to simulate human sweat, and the obtained solution was then dropped like sweat on human-cadaver skin. The human-cadaver skin was then covered with the sensing patch and, after two hours, the SERS spectra were measured. Despite the good potential as a POC device and the ability to accumulate molecules in the SFF layer, so that the analysis can be performed long after the molecule has been released in the sweat, the wearable SERS patch cannot be used for real-time monitoring, because analytes molecules took about 1,5 h to reach the AgNWs layer, so that the analysis is not very fast.

#### 7.4. Multiplexed Analysis with SERS Nanotags

Acute myocardial infarction (AMI) is recognized as one of the most immediately life-threatening problems and it is among the main causes of death in the world; for its quick diagnosis, the simultaneous detection of cardiac biomarkers such as cardiac troponin I (cTnI), creatine kinase-MB isoenzymes (CK-MB) and myoglobin (Myo) is required. On this basis, lives could be more easily saved by elevating the level in AMI tracking through the multiplex and quantitative detection of these three biomarkers performed with a rapid LFA strip test. Taking into account the increasing interest in the production of SERS nanotags for rapid and accurate analysis, Zhang, in his work [73], developed an LFA strip for the multiplexed and quantitative detection of the three cardiac biomarkers for early AMI diagnosis integrating a specifically created SERS nanotag. The SERS LFA strip is formed by five components: a backing pad, a sample pad, a conjugate pad, a nitrocellulose (NC) membrane and an adsorbing pad. To the lower part of the backing pad are fixed the sample and the conjugate pad; the NC membrane is fixed to the middle part of the backing pad whereas to the higher part is fixed the adsorbing pad. To provide a continuous stream of the developing solution from the sample to the adsorption pad by means of capillary forces, the components are overlapped. In the conjugate pad are the Myo, cTnI, and CK-MB detection antibody conjugated with the SERS nanotags. In place of gold colloid, silver-gold core-shell bimetallic nanotags encapsulating Nile blue A (NBA) molecules (the Raman reports) in the interior gap between the two metals (AgNBA@Au) were synthesised as SERS nanotags. Onto the NC membrane were placed the three test lines and the control line: the test lines were prepared by separately spotting to capture the antibody against CK-MB, the capture antibody against Myo and the capture antibody against cTnI, while the control line was produced with goat anti-mouse IgG. To collect the SERS spectra coming from the SERS nanotags conjugated with the analyte in the test line, a linear dynamic range (LDR) of 0.01–500 ng mL<sup>-1</sup>, 0.01–50 ng mL<sup>-1</sup>, and 0.02–90 ng mL<sup>-1</sup> is needed for Myo, cTnI, and CK-MB. With results comparable with chemiluminescence immunoassay (CLIA) and its ease of use arising from pre-treatments not being required, the sensitive SERS LFA strips hold great potential for point-of-care testing technologies (POCT) for AMI diagnosis with applications in health monitoring and clinical alerts. In a later work [74], the authors developed a test strip with a single test line comprising the capture antibodies against the

three cardiac biomarkers CK-MB, cTnI, and Myo with the aim to improve the performances of the devices by reducing the analysis time. In Table 1 a comparison of the considered POC devices has been reported.

**Table 1.** Comparison of the advantages and limitations of the considered POC devices.

System	Analyte	Advantages	Limitations	Reference
Colorimetric sensing of urea based on the generation of silver nanoparticles performed through image analysis with a smartphone.	Urea.	-High selectivity toward various interferents in human urine. -High sensitivity. -Wide detection range. -No need for complicated instrumentation. -Real-time responses.	-	[60]
Ironphone system.	Ferritin.	-High sensitivity. -Real-time response. -No need for bulky equipment.	Ready as POC device.	[61]
Nutriphone system.	Vitamin B <sub>12</sub> .	-High sensitivity. -Real-time response. -No need for bulky equipment.	Ready as POC device.	[62]
Smartphone lateral flow point-of-care test for Ebola virus.	Ebola virus.	-High sensitivity and specificity. -Rapid and portable analysis. -Data storage and sharing as well as geographical tagging of the tested individuals.	Further work to evaluate sensitivity and specificity in larger cohort groups, need for studies on assay compatibility under a broader range of environmental conditions at POC and vaccine evaluation.	[63]
Lateral flow assays based on AuNPs.	-Normal KRAS gene and three of the most significant/common mutations in the KRAS gene in cell-free DNA.	-High detectability. -Good specificity. -Good reproducibility. -Visual detection. -Low cost. -Rapid analysis time.	The whole protocol includes techniques such as DNA isolation, polymerase chain reaction (PCR) and Primer extension reaction (PEXT), requiring trained personnel.	[68]
Gold nanorods in solution.	-KRAS gene associated with pancreatic ductal adenocarcinoma in circulating tumor DNA (ctDNA).	-High sensitivity.	-Need for bulky instrumentation such as UV-spectrometer.	[69]
Wearable plasmonic paper-based microfluidic device for continuous analysis of sweat.	-Uric acid (UA) in sweat at physiological and pathological concentrations.	-Continuous, real-time, label-free analysis of biomolecules. -Performances not compromised by the poor stability of biorecognition elements -High sensitivity -High specificity	-Need for an optimized miniaturized Raman spectrometer as read-out system.	[71]

Table 1. Cont.

System	Analyte	Advantages	Limitations	Reference
SERS patch sensor based on plasmonic silver nanowire (AgNW).	2-fluoromethamphetamine (2-FMA).	-Excellent skin biocompatibility. -Flexibility. -Durability for use as a wearable sensor. -High sensitivity. -High specificity. -Direct label-free detection.	-Need for a miniaturized Raman spectrometer. -Quasi real-time monitoring: necessity to wait more than 90 min to start analysis.	[72]
Core-shell SERS nanotag-based multiplex LFA (SERS LFA) for rapid and quantitative detection of three cardiac biomarkers.	-cardiac troponin I (cTnI). -creatine kinase-MB isoenzymes (CK-MB). -myoglobin (Myo).	-Ultrasensitive. -Fast. -Low cost. -Easy to use. -Free of sample pretreatment and professional labors.	-Need for a miniaturized and portable Raman spectrometer, but they still must be improved.	[73]
Core-shell SERS nanotag-based multiplex LFA (SERS LFA) for rapid and quantitative detection of three cardiac biomarkers.	-cardiac troponin I (cTnI). -creatine kinase-MB isoenzymes (CK-MB). -myoglobin (Myo).	-Ultrasensitive. -Faster quantification of three cardiac biomarkers. -Low cost. -Easy to use. -Free of sample pretreatment and professional labor.	-Need for a miniaturized and portable Raman spectrometer, but they still must be improved.	[74]

## 8. Summary and Outlook

This work outlined the growing interest in developing POC platforms based on plasmonic sensing platforms to create devices with great potential to be implemented as next-generation diagnostic tools. In order to gain a better understanding of the novel sensing transducers, firstly, the optical properties of plasmonic metal nanoparticles were reviewed, and then the key issues of the POC devices were discussed. It was illustrated that the microfluidics of the system is a critical point to integrate the plasmonic transducer into a POC device and the attention was focused on LFA and  $\mu$ PADs, for their simplicity arising from the lack of a need for external forces such as micropumps and their low-cost. In addition, it was illustrated how common technologies, such as smartphones, and analytical methodologies, such as SERS, are considered intriguing readout systems in view of their ability to provide quantitative analysis, a key point for timely and highly precise diagnostics. For an accurate prognosis and treatment evaluation, the determination of multiple biomarkers at the same time is central so the strategies developed for the multiplexed analysis were also discussed. Finally, several applications of POC devices were reported, such as in liquid biopsy, wearable sensors and smartphone-assisted devices. The objective of the work is a critical discussion of the progress achieved in developing POC devices: while the interest in new nanomaterials such as hybrid composites of plasmonic metal nanoparticles and 2D nanomaterials creates new possibilities for the creation of new sensing transducers, the route towards their effective implementation as commercial biosensing platforms still has limitations that must be overcome. One of the critical challenges in the development of POC devices, for example, are the SERS readers: they are not very user-friendly, need long time to acquire data, and have a high cost. In addition, the results obtained from SERS are not easily understood, so that, for applications in the real world where the analysis is performed by untrained people, it is necessary to develop a software able to accurately and reliably process, interpret, and report the results in a way that they are simple to understand. In this scenario, some work must be performed to develop handheld a Raman spectrometer which gives a simple-to-understand readout to be integrated into POC devices. Still, despite SERS technology having great potential, its use in clinical diagnostics is not approved

because of the reproducibility of SERS substrates and the complexity of the equipment, which limits a great number of applications. Efforts are directed towards the creation of a “closed case” system for the final user, where the sample to be determined is introduced and analysed and the results generated on a quantified, reliable and simple readout system; this will enable the widespread use of this technology as commercial biosensing platforms. In addition, another one of the main challenges to face in the development of the next generation of biosensing diagnostic devices is their integration into eHealth systems and, in this context, the technological developments in the field of Internet of medical things (IoMT) are becoming more important; these offer wireless-based operation and the connectivity of POC devices with health experts and medical centres. During recent years, POC platforms have also been integrated with machine-learning (ML) algorithms, such as artificial intelligence (AI), resulting in a new model of making decisions based on data analytics. Firstly, the AI sensors analyse the sample using portable instruments which are then able to automatically digitalize the detected biomarker concentration. Successively, on the basis of the acquired data, the disease spectrum can be predicted by means of algorithms such as classification, cluster, and pattern, to make decisions. In this context, AI is proving to be a promising tool for providing medical practitioners a further possibility in terms of personal treatment and observations of their outcomes. The use of health analytics, such as IoMT and AI, thus, contributes to personalised care for the active management and prevention of disease risk, improving the wellness of the patient. The greatest breakthrough of the next generation of diagnostic tools will be the realization of so-called P6 medicine (personalized, predictive, preventive, participatory, psycho cognitive, and public), and, ultimately, also a contribution to the achievement of cancer chronology, as a further step in the fight against the disease.

**Author Contributions:** Conceptualization, methodology, writing—original draft preparation, writing—review and editing C.S., A.F. and E.C.B.A.A.; visualization, C.S.; funding acquisition, A.F., E.C.B.A.A. and M.V. All authors have read and agreed to the published version of the manuscript.

**Funding:** This research was supported by Portuguese national funds provided by FCT—Fundação para a Ciência e Tecnologia, through grant SFRH/BD/09347/2021, and 2022.02069.PTDC, 2022.07694.PTDC, UIDB/EEA/00066/2020, UIDP/EEA/00066/2020, LA/P/0104/2020 and by Instituto Politecnico de Lisboa through project IPL/2022/Metalogic\_ISEL.

**Data Availability Statement:** No new data were created.

**Conflicts of Interest:** The authors declare no conflict of interest.

## References

1. Buddhadev, P.; Pramod, R.V.; Nagaraj, P.S.; Pranjal, C. Biosensor nanoengineering: Design, operation, and implementation for biomolecular analysis. *Sens. Int.* **2020**, *1*, 100040.
2. Smith, S.; Korvink, J.G.; Mager, D.; Land, K. The potential of paper-based diagnostics to meet the ASSURED criteria. *RSC Adv.* **2018**, *8*, 34012–34034. [[CrossRef](#)] [[PubMed](#)]
3. Yang, S.-M.; Lv, S.; Zhang, W.; Cui, Y. Microfluidic Point-of-Care (POC) Devices in Early Diagnosis: A Review of Opportunities and Challenges. *Sensors* **2022**, *22*, 1620. [[CrossRef](#)] [[PubMed](#)]
4. Conde, J.P.; Madaboosi, N.; Soares, R.R.G.; Fernandes, J.T.S.; Novo, P.; Moulas, G.; Chu, V. Lab-on-chip systems for integrated bioanalyses. *Essays Biochem.* **2016**, *60*, 121–131.
5. Özyurt, C.; Uludağ, İ.; İnce, B.; Sezgintürk, M.K. Lab-on-a-chip systems for cancer biomarker diagnosis. *J. Pharm. Biomed. Anal.* **2023**, *226*, 115266. [[CrossRef](#)]
6. Laghari, A.A.; Wu, K.; Laghari, R.A.; Ali, M.; Khan, A.A. A Review and State of Art of Internet of Things (IoT). *Arch. Comput. Methods Eng.* **2022**, *29*, 1395–1413. [[CrossRef](#)]
7. Thilakarathne, N.N.; Kagita, M.K.; Gadekallu, D.T.R. The Role of the Internet of Things in Health Care: A Systematic and Comprehensive Study. *Int. J. Eng. Manag. Res.* **2020**, *10*, 145–159. [[CrossRef](#)]
8. Habibzadeh, H.; Dinesh, K.; Shishvan, O.R.; Boggio-Dandry, A.; Sharma, G.; Soyata, T. A Survey of Healthcare Internet of Things (HIoT): A Clinical Perspective. *IEEE Internet Things J.* **2020**, *7*, 53–71. [[CrossRef](#)]
9. Chen, Y.; Ming, H. Review of surface plasmon resonance and localized surface plasmon resonance sensor. *Photonic Sens.* **2012**, *2*, 37–49. [[CrossRef](#)]

10. Estevez, M.C.; Otte, M.A.; Sepulveda, B.; Lechuga, L.M. Trends and challenges of refractometric nanoplasmonic biosensors: A review. *Anal. Chim. Acta* **2014**, *806*, 55–73. [[CrossRef](#)]
11. González, A.L.; Noguez, C. Optical properties of silver nanoparticles. *Phys. Status Solidi (C) Curr. Top. Solid State Phys.* **2007**, *4*, 4118–4126. [[CrossRef](#)]
12. Liz-Marzán, L.M. Tailoring Surface Plasmons through the Morphology and Assembly of Metal Nanoparticles. *Langmuir* **2006**, *22*, 32–41. [[CrossRef](#)]
13. Jain, P.K.; Huang, X.; El-Sayed, I.H.; El-Sayed, M.A. Noble Metals on the Nanoscale: Optical and Photothermal Properties and Some Applications in Imaging, Sensing, Biology, and Medicine. *Acc. Chem. Res.* **2008**, *41*, 1578–1586. [[CrossRef](#)]
14. Drozdov, A.; Andreev, M.; Kozlov, M.; Petukhov, D.; Klimonsky, S.; Pettinari, C. Lycurgus cup: The nature of dichroism in a replica glass having similar composition. *J. Cult. Herit.* **2021**, *51*, 71–78. [[CrossRef](#)]
15. Serafinelli, C.; Fantoni, A.; Alegria, E.C.B.A.; Vieira, M. Hybrid Nanocomposites of Plasmonic Metal Nanostructures and 2D Nanomaterials for Improved Colorimetric Detection. *Chemosensors* **2022**, *10*, 237. [[CrossRef](#)]
16. Mejía-Salazar, J.R.; Cruz, K.R.; Vásques, E.M.M.; de Oliveira, O.N., Jr. Microfluidic Point-of-Care Devices: New Trends and Future Prospects for eHealth Diagnostics. *Sensors* **2020**, *20*, 1951. [[CrossRef](#)] [[PubMed](#)]
17. Koczula, K.M. Lateral flow assays. *Essays Biochem.* **2016**, *60*, 111–120. [[PubMed](#)]
18. Zhou, W.; Dou, M.; Timilsina, S.S.; Xu, F.; Li, X. Recent innovations in cost-effective polymer and paper hybrid microfluidic devices. *Lab A Chip* **2021**, *21*, 2658–2683. [[CrossRef](#)] [[PubMed](#)]
19. Tseng, C.-C.; Kung, C.-T.; Chen, R.-F.; Tsai, M.-H.; Chao, H.-R.; Wang, Y.-N.; Fu, L.-M. Recent advances in microfluidic paper-based assay devices for diagnosis of human diseases using saliva, tears and sweat samples. *Sens. Actuators B Chem.* **2021**, *342*, 130078. [[CrossRef](#)]
20. Müller, R.H.; Clegg, D.L. Automatic Paper Chromatography. *Anal. Chem.* **1949**, *21*, 1123–1125. [[CrossRef](#)]
21. Martinez, A.W.; Phillips, S.T.; Whitesides, G.M. Diagnostics for the Developing World: Microfluidic Paper-Based Analytical Devices. *Anal. Chem.* **2010**, *82*, 3–10. [[CrossRef](#)]
22. Quesada-González, D.; Merkoçi, A. Mobile phone-based biosensing: An emerging “diagnostic and communication” technology. *Biosens. Bioelectron.* **2017**, *92*, 549–562. [[CrossRef](#)]
23. Wei, Q.; Qi, H.; Luo, W.; Tseng, D.; Ki, S.J.; Wan, Z.; Göröcs, Z.; Bentolila, L.A.; Wu, T.-T.; Sun, R.; et al. Fluorescent Imaging of Single Nanoparticles and Viruses on a Smart Phone. *ACS Nano* **2013**, *7*, 9147–9155. [[CrossRef](#)]
24. Smith, Z.J.; Chu, K.; Espenson, A.R.; Rahimzadeh, M.; Gryshuk, A.; Molinaro, M.; Dwyre, D.M.; Lane, S.; Matthews, D.; Wachsmann-Hogiu, S. Cell-Phone-Based Platform for Biomedical Device Development and Education Applications. *PLoS ONE* **2011**, *6*, e17150. [[CrossRef](#)]
25. Wang, Y.; Liu, X.; Chen, P.; Tran, N.T.; Zhang, J.; Chia, W.S.; Boujday, S.; Liedberg, B. Smartphone spectrometer for colorimetric biosensing. *Analyst* **2016**, *141*, 3233–3238. [[CrossRef](#)]
26. Fantoni, A.; Vygranenko, Y.; Maçarico, A.; Serafinelli, C.; Fernandes, M.; Mansour, R.; Jesus, R.; Vieira, M. Arrayed graphene enhanced surface plasmon resonance for sensing applications. In Proceedings of the SPIE, Optical Components and Materials XVIII, Bellingham, WA, USA, 6–11 March 2021; Volume 11682, pp. 1–5.
27. Lin, L.; Bi, X.; Gu, Y.; Wang, F.; Ye, J. Surface-enhanced Raman scattering nanotags for bioimaging. *J. Appl. Phys.* **2021**, *129*, 191101. [[CrossRef](#)]
28. Fleischmann, M.; Hendra, P.J.; Quillan, A.J.M. Raman spectra of pyridine adsorbed at a silver electrode. *Chem. Phys. Lett.* **1974**, *26*, 163–166. [[CrossRef](#)]
29. Liz-Marzán, L.M. Present and Future of Surface-Enhanced Raman Scattering. *ACS Nano* **2020**, *14*, 28–117.
30. Serafinelli, C.; Fantoni, A.; Alegria, E.C.B.A.; Vieira, M. Plasmonic Metal Nanoparticles Hybridized with 2D Nanomaterials for SERS Detection: A Review. *Biosensors* **2022**, *12*, 225. [[CrossRef](#)]
31. Oliverio, M.; Perotto, S.; Messina, G.C.; Lovato, L.; De Angelis, F. Chemical Functionalization of Plasmonic Surface Biosensors: A Tutorial Review on Issues, Strategies, and Costs. *ACS Appl. Mater. Interfaces* **2017**, *9*, 29394–29411. [[CrossRef](#)]
32. Kurt, H.; Pishva, P.; Pehlivan, Z.S.; Arsoy, E.G.; Saleem, Q.; Bayazit, M.K.; Yüce, M. Nanoplasmonic biosensors: Theory, structure, design, and review of recent applications. *Anal. Chim. Acta* **2021**, *1185*, 338842. [[CrossRef](#)] [[PubMed](#)]
33. Sharma, S.; Byrne, H.; O’Kennedy, R.J. Antibodies and antibody-derived analytical biosensors. *Essays Biochem.* **2016**, *60*, 9–18. [[PubMed](#)]
34. Morales, M.A.; Halpern, J.M. Guide to Selecting a Biorecognition Element for Biosensors. *Bioconjugate Chem.* **2018**, *29*, 3231–3239. [[CrossRef](#)] [[PubMed](#)]
35. Reimhult, E.; Höök, F. Design of Surface Modifications for Nanoscale Sensor Applications. *Sensors* **2015**, *15*, 1635–1675. [[CrossRef](#)]
36. Leibl, N.; Haupt, K.; Gonzato, C.; Duma, L. Molecularly Imprinted Polymers for Chemical Sensing: A Tutorial Review. *Chemosensors* **2021**, *9*, 123. [[CrossRef](#)]
37. Zahavi, D.; Weiner, L. Monoclonal Antibodies in Cancer Therapy. *Antibodies* **2020**, *9*, 34. [[CrossRef](#)]
38. Melani, R.D.; Srzentić, K.; Gerbasi, V.R.; McGee, J.P.; Huguet, R.; Fornelli, L. Direct measurement of light and heavy antibody chains using ion mobility and middle-down mass spectrometry. *mAbs* **2019**, *11*, 1351–1357. [[CrossRef](#)]
39. Wang, Q.; Chen, Y.; Park, J.; Liu, X.; Hu, Y.; Wang, T.; McFarland, K.; Betenbaugh, M.J. Design and Production of Bispecific Antibodies. *Antibodies* **2019**, *8*, 43. [[CrossRef](#)]

40. Chiu, M.L.; Goulet, D.R.; Teplyakov, A.; Gilliland, G.L. Antibody Structure and Function: The Basis for Engineering Therapeutics. *Antibodies* **2019**, *8*, 55. [[CrossRef](#)]
41. Le Basle, Y.; Chennell, P.; Tokhadze, N.; Astier, A.; Sautou, V. Physicochemical Stability of Monoclonal Antibodies: A Review. *J. Pharm. Sci.* **2020**, *109*, 169–190. [[CrossRef](#)]
42. Suurs, F.V.; Hooge, M.N.L.-D.; de Vries, E.G.E.; Jan, A.D. A review of bispecific antibodies and antibody constructs in oncology and clinical challenges. *Pharmacol. Ther.* **2019**, *201*, 103–119. [[CrossRef](#)]
43. Bates, A.; Power, C.A. David vs. Goliath: The Structure, Function, and Clinical Prospects of Antibody Fragments. *Antibodies* **2019**, *8*, 28. [[CrossRef](#)]
44. Wang, Y.; Xianyu, Y. Nanobody and Nanozyme-Enabled Immunoassays with Enhanced Specificity and Sensitivity. *Small Methods* **2022**, *6*, 2101576. [[CrossRef](#)]
45. Li, B.; Qin, X.; Mi, L.-Z. Nanobodies: From structure to applications in non-injectable and bispecific biotherapeutic development. *Nanoscale* **2022**, *14*, 7110–7122. [[CrossRef](#)]
46. Jovčevska, I.; Muyldermans, S. The Therapeutic Potential of Nanobodies. *BioDrugs* **2020**, *34*, 11–26. [[CrossRef](#)]
47. Simões, B.; Guedens, W.J.; Keene, C.; Kubiak-Ossowska, K.; Mulheran, P.; Kotowska, A.M.; Scurr, D.J.; Alexander, M.R.; Broisat, A.; Johnson, S.; et al. Direct Immobilization of Engineered Nanobodies on Gold Sensors. *ACS Appl. Mater. Interfaces* **2021**, *13*, 17353–17360. [[CrossRef](#)] [[PubMed](#)]
48. Goossens, J.; Sein, H.; Lu, S.; Radwanska, M.; Muyldermans, S.; Sterckx, Y.G.-J.; Magez, S. Functionalization of gold nanoparticles with nanobodies through physical adsorption. *Anal. Methods* **2017**, *9*, 3430–3440. [[CrossRef](#)]
49. Alsadig, A.; Abbasgholi-NA, B.; Vondracek, H.; Medagli, B.; Fortuna, S.; Posocco, P.; Parisse, P.; Cabrera, H.; Casalis, L. DNA-Directed Protein Anchoring on Oligo/Alkanethiol-Coated Gold Nanoparticles: A Versatile Platform for Biosensing Applications. *Nanomaterials* **2023**, *13*, 78. [[CrossRef](#)] [[PubMed](#)]
50. Zhang, C.; Wang, Y.; Liu, Z.; Bai, M.; Wang, J.; Wang, Y. Nanobody-based immunochromatographic biosensor for colorimetric and photothermal dual-mode detection of foodborne pathogens. *Sens. Actuators B Chem.* **2022**, *369*, 132371. [[CrossRef](#)]
51. Huang, L.; Tian, S.; Zhao, W.; Liu, K.; Ma, X.; Guo, J. Multiplexed detection of biomarkers in lateral-flow immunoassays. *Analyst* **2020**, *145*, 2828–2840. [[CrossRef](#)]
52. Liu, X.; Wu, W.; Cui, D.; Chen, X.; Li, W. Functional Micro-/Nanomaterials for Multiplexed Biodetection. *Adv. Mater.* **2021**, *33*, 2004734. [[CrossRef](#)]
53. Jarockyte, G.; Karabanovas, V.; Rotomskis, R.; Mobasheri, A. Multiplexed Nanobiosensors: Current Trends in Early Diagnostics. *Sensors* **2020**, *20*, 6890. [[CrossRef](#)]
54. PrJamkhande, G.; Ghule, N.W.; Bamer, A.H.; Kalaskar, M.G. Metal nanoparticles synthesis: An overview on methods of preparation, advantages and disadvantages, and applications. *J. Drug Deliv. Sci. Technol.* **2019**, *53*, 101174. [[CrossRef](#)]
55. Goodacre, R.; Graham, D.; Faulds, K. Recent developments in quantitative SERS: Moving towards absolute quantification. *Trends Anal. Chem.* **2018**, *102*, 359–368. [[CrossRef](#)]
56. Fabris, L. Gold-based SERS tags for biomedical imaging. *J. Opt.* **2015**, *17*, 114002. [[CrossRef](#)]
57. Lenzi, E.; de Aberasturi, D.J.; Liz-Marzán, L.M. Surface-Enhanced Raman Scattering Tags for Three-Dimensional Bioimaging and Biomarker Detection. *ACS Sens.* **2019**, *4*, 1126–1137. [[CrossRef](#)]
58. Sena-Torralba, A.; Álvarez-Diduk, R.; Parolo, C.; Piper, A.; Merkoçi, A. Toward Next Generation Lateral Flow Assays: Integration of Nanomaterials. *Chem. Rev.* **2022**, *122*, 14881–14910. [[CrossRef](#)]
59. Liu, Y.; Zhang, X. Microfluidics-Based Plasmonic Biosensing System Based on Patterned Plasmonic Nanostructure Arrays. *Micromachines* **2021**, *12*, 826. [[CrossRef](#)]
60. Choi, C.-K.; Shaban, S.M.; Moon, B.-S.; Pyun, D.-G.; Kim, D.-H. Smartphone-assisted point-of-care colorimetric biosensor for the detection of urea via pH-mediated AgNPs growth. *Anal. Chim. Acta* **2021**, *1170*, 338630. [[CrossRef](#)]
61. Srinivasan, B.; O'Dell, D.; Finkelstein, J.L.; Lee, S.; Erickson, D.; Mehta, S. ironPhone: Mobile device-coupled point-of-care diagnostics for assessment of iron status by quantification of serum ferritin. *Biosens. Bioelectron.* **2018**, *99*, 115–121. [[CrossRef](#)]
62. Lee, S.; O'Dell, D.; Hohenstein, J.; Colt, S.; Mehta, S.; Erickson, D. NutriPhone: A mobile platform for low-cost point-of-care quantification of vitamin B12 concentrations. *Sci. Rep.* **2016**, *6*, 28237. [[CrossRef](#)] [[PubMed](#)]
63. Brangel, P.; Sobarzo, A.; Parolo, C.; Miller, B.S.; Howes, P.D.; Gelkop, S.; Lutwama, J.J.; Dye, J.M.; McKendry, R.A.; Lobel, L.; et al. A Serological Point-of-Care Test for the Detection of IgG Antibodies against Ebola Virus in Human Survivors. *ACS Nano* **2018**, *12*, 63–73. [[CrossRef](#)] [[PubMed](#)]
64. Poulet, G.; Massias, J.; Taly, V. Liquid Biopsy: General Concepts. *Acta Cytol.* **2019**, *63*, 449–455. [[CrossRef](#)] [[PubMed](#)]
65. Alix-Panabières, C. Liquid Biopsy: From Discovery to Clinical Application. *Cancer Discov.* **2021**, *11*, 858–873. [[CrossRef](#)] [[PubMed](#)]
66. Abalde-Cela, S.; Wu, L.; Teixeira, A.; Oliveira, K.; Diéguez, L. Multiplexing Liquid Biopsy with Surface-Enhanced Raman Scattering Spectroscopy. *Adv. Opt. Mater.* **2021**, *9*, 2001171. [[CrossRef](#)]
67. Moisoiu, V.; Iancu, S.D.; Stefanu, A.; Moisoiu, T.; Pardini, B.; Dragomir, M.P.; Crisan, N.; Avram, L.; Crisan, D.; Andras, I.; et al. SERS liquid biopsy: An emerging tool for medical diagnosis. *Colloids Surf. B Biointerfaces* **2021**, *208*, 112064. [[CrossRef](#)]
68. Kalligosfyri, P.; Nikou, S.; Bravou, V.; Kalogianni, D.P. Liquid biopsy genotyping by a simple lateral flow strip assay with visual detection. *Anal. Chim. Acta* **2021**, *1163*, 338470. [[CrossRef](#)]
69. Tadimety, A.; Zhang, Y.; Kready, K.M.; Palinski, T.J.; Tsongalis, G.J.; Zhang, J.X. Design of peptide nucleic acid probes on plasmonic gold nanorods for detection of circulating tumor DNA point mutations. *Biosens. Bioelectron.* **2019**, *130*, 236–244. [[CrossRef](#)]

70. Kinugasa, H.; Nouse, K.; Miyahara, K.; Morimoto, Y.; Dohi, C.; Tsutsumi, K.; Kato, H.; Matsubara, T.; Okada, H.; Yamamoto, K. Detection of K-ras gene mutation by liquid biopsy in patients with pancreatic cancer. *Cancer* **2015**, *121*, 2271–2280. [[CrossRef](#)]
71. Mogera, U.; Guo, H.; Namkoong, M.; Rahman, M.S.; Nguyen, T.; Tian, L. Wearable plasmonic paper-based microfluidics for continuous sweat analysis. *Sci. Adv.* **2022**, *8*, eabn1736. [[CrossRef](#)]
72. Koh, E.H.; Lee, W.-C.; Choi, Y.-J.; Moon, J.-I.; Jang, J.; Park, S.-G.; Choo, J.; Kim, D.-H.; Jung, H.S. A Wearable Surface-Enhanced Raman Scattering Sensor for Label-Free Molecular Detection. *ACS Appl. Mater. Interfaces* **2021**, *13*, 3024–3032. [[CrossRef](#)] [[PubMed](#)]
73. Zhang, D.; Huang, L.; Liu, B.; Ni, H.; Sun, L.; Su, E.; Chen, H.; Gu, Z.; Zhao, X. Quantitative and ultrasensitive detection of multiplex cardiac biomarkers in lateral flow assay with core-shell SERS nanotags. *Biosens. Bioelectron.* **2018**, *106*, 204–211. [[CrossRef](#)] [[PubMed](#)]
74. Zhang, D.; Huang, L.; Liu, B.; Su, E.; Chen, H.-Y.; Gu, Z.; Zhao, X. Quantitative detection of multiplex cardiac biomarkers with encoded SERS nanotags on a single T line in lateral flow assay. *Sens. Actuators B Chem.* **2018**, *277*, 502–509. [[CrossRef](#)]

**Disclaimer/Publisher's Note:** The statements, opinions and data contained in all publications are solely those of the individual author(s) and contributor(s) and not of MDPI and/or the editor(s). MDPI and/or the editor(s) disclaim responsibility for any injury to people or property resulting from any ideas, methods, instructions or products referred to in the content.